Synthesis of polyoxovanadates via "chimie douce"

Jacques Livage *

*Chimie de la Matière Condensée, Institut Universitaire de France,
Université Pierre et Marie Curie, 4 place Jussieu, 75252 Paris, France*

Contents

Abstract

A large variety of new polyoxovanadates have been synthesized during the past few years by sol–gel chemistry or hydrothermal methods. These wet chemistry methods offer many advantages compared to the usual solid state syntheses. New open structures have been obtained from aqueous precursors. They result from the self-assembling of ionic species in the solution.

Vanadium oxide gels and sols, $V_2O_5 \cdot nH_2O$, are formed around the point of zero charge (pH ≈ 2). They have a ribbon-like structure and exhibit a liquid crystal behavior. These mesophases are similar to those currently observed with nematic polymers. Xerogel layers deposited from $V_2O_5 \cdot nH_2O$ gels exhibit some preferred orientation and behave as versatile host structures for intercalation giving new hybrid organic–inorganic nanocomposites.

Layered structures are formed around pH ≈ 7 in the presence of large organic cations. They are built of mixed valence polyoxovanadate planes made of $[VO_5]$ pyramids and $[VO_4]$ tetrahedra. Organic cations lie between the oxide layers where they interact with the negative oxygen of the V=O double bonds.

* Corresponding author. Fax: + 33 1 44 27 47 69; e-mail: livage@ccr.jussieu.fr

Anions can behave as templating agents. Hollow cluster shells are formed around anions that remain encapsulated within the negatively charged polyvanadate cage. Large cations only behave as counter ions for the formation of a neutral crystalline network.

It appears that the molecular structure of V^V precursors depends mainly on pH, but the way they self-assemble may be governed by other ionic species in the solution. © 1998 Elsevier Science S.A. All rights reserved.

Keywords: Hydrothermal syntheses; Mesophases; Sol–gel; Templates; Vanadates

1. Introduction

The synthesis of oxide materials via solid state reactions is usually performed at high temperature. Only strong iono-covalent bonds are then involved in the formation of the compound, leading to dense thermodynamically stable phases. Chemical syntheses via "chimie douce" have been widely developed during the past decade [1]. They currently involve wet chemistry methods such as coprecipitation, sol–gel chemistry or hydrothermal syntheses, and often lead to metastable phases with open structures. The presence of a liquid phase, usually an aqueous solution, favors the diffusion of small ionic or molecular species. Homogeneous mixing of the precursors is then obtained in the solution at the molecular level so that multicomponent materials can be formed at much lower temperature.

One of the main advantages of wet chemistry methods is that weak interactions (hydrogen bonds, van der Waals, hydrophilic–hydrophobic interactions, etc.) are not broken at low temperature. They are involved in the self-assembling of molecular precursors and can play an important role during the formation of the oxide network. Subtle changes in chemical conditions (pH, counter ion, template, etc.) lead to new supramolecular associations and therefore to different nanostructures.

The aqueous chemistry of vanadium, V^V, provides a good example of the numerous possibilities offered by "chimie douce" syntheses. Vanadium in its higher oxidation states gives many isopolyvanadates that exhibit a large variety of structures, ranging from chain metavanadates $[VO_3^-]_n$, to layered oxides $[V_2O_5]$ and compact polyanions $[V_{10}O_{28}]^{6-}$ [2]. Even polyanionic hollow cages such as $[V_{15}O_{36}]^{5-}$ in which anions are encapsulated have been reported [3]. Such a rich structural chemistry is due to the ability of vanadium to adopt a variety of coordination geometries, $[VO_6]$, $[VO_5]$, $[VO_4]$ and oxidation states (V^V, V^{IV}). A large number of nice papers have been published during these past years, mainly by the groups of A. Müller, J. Zubieta and R.C. Haushalter, reporting the synthesis of new polyoxovanadates.

Therefore, this paper is not intended to give an extensive description of the field; excellent reviews have been published recently [3–6]. We would like to discuss the main chemical processes involved in the formation of a polyoxovanadate network from an aqueous solution. For simplicity, the discussion is restricted to systems leading to a vanadium oxide network in which only V–O–V bonds are observed. Heteropolyvanadates incorporating phosphate, arsenate, borate or other transition metal cations will not be discussed.

2. Hydrolysis of V^V in aqueous solutions

A large variety of V^V species can be found in aqueous solutions [7]. At room temperature they mainly depend on vanadium concentration and pH. When dissolved in water, V^{5+} ions are surrounded by dipolar water molecules giving $[V(OH_2)_6]^{5+}$ solvated species. However, due to the strong polarizing power of V^{5+} and the Lewis acid properties of H_2O, some electron transfer occurs from the $3a_1$ orbital of the water molecule toward the empty 3d orbitals of V^{5+} (electronic configuration $3d^0$). This "σ" transfer decreases the electron density within the bonding orbitals of H_2O and weakens O–H bonds. Coordinated water molecules become more acidic and deprotonation occurs spontaneously as follows:

$$[V(OH_2)_6]^{5+} + hH_2O \Rightarrow [V(OH)_h(OH_2)_{6-h}]^{(5-h)+} + hH_3O^+ \qquad (1)$$
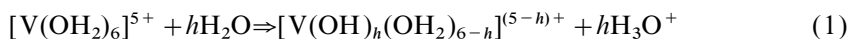
The hydrolysis ratio h increases with pH, leading to the formation of aquo, hydroxo or oxo species [Fig. 1(a)]. It can be predicted theoretically in the frame of the partial charge model developed by M. Henry in Paris [8]. Extending the electronegativity equalization principle of Sanderson [9], we may assume that deprotonation [Eq. (1)] goes on until the mean electronegativity of the V^V precursor "$[V(OH)_h(OH_2)_{6-h}]^{(5-h)+}$" becomes equal to that of the aqueous solution. Moreover, we have shown that the mean electronegativity of an aqueous solution, χ_{aq}, could be expressed as a linear function of pH [8]:

$$\chi_{aq} = 2.732 - 0.035 pH \qquad (2)$$

It is then possible to work out the mean electronegativity, χ_v, of the V^V precursor at a given pH and then the hydrolysis ratio h as a function of pH [Fig. 1(b)].

Deprotonation is favored by the high oxidation state of V^{5+}, and $[V(OH_2)_6]^{5+}$ species cannot be observed in aqueous solutions even at very low pH. The hydrolysis ratio actually increases from $h = 4$ to $h = 12$ in the pH range 0–14. The less deprotonated species at pH 0 should correspond to the $[V(OH)_4(OH_2)_2]^+$ precursor ($h = 4$). However, some internal proton transfer between adjacent OH groups occurs in order to decrease the positive charge of V^V via the formation of V=O double bonds. The stable form at low pH (pH<2) is then the solvated cis-dioxo cation $[VO_2(OH_2)_4]^{2+}$, usually written as $[VO_2]^+$.

It has to be pointed out that, as deprotonation goes on, the electron transfer from coordinated oxygen atoms toward the empty 3d orbitals of the V^V atom increases, therefore decreasing the positive partial charge of vanadium. The V–O bond becomes more covalent and the coordination of V^V decreases from six to four, giving the tetrahedral vanadate anion $[VO_4]^{3-}$ that is the stable form above pH 13. This coordination change occurs around pH≈6. It can easily be seen with the naked eyes, as six-fold coordinated V^V gives a yellow–orange coloration whereas tetrahedral $[VO_4]$ is colorless [10].

Actually, monomeric species can only be observed in very diluted solutions ($c < 10^{-4}$ mol l^{-1}). In more concentrated solutions, condensation occurs in the pH range where V–OH groups are formed ($2 \leqslant pH \leqslant 13$) (Fig. 1). Two main reactions
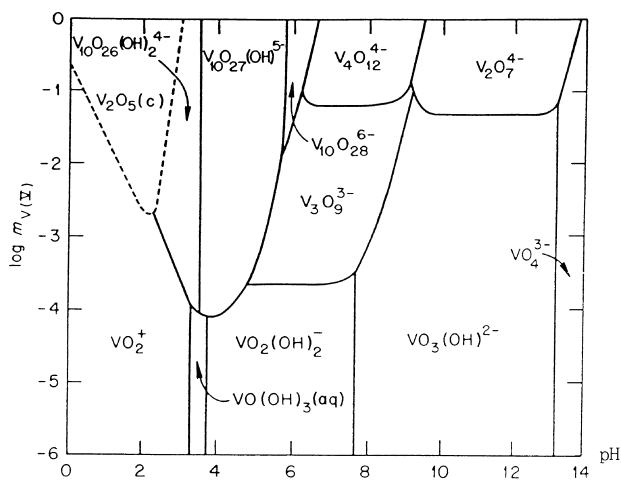
(a)
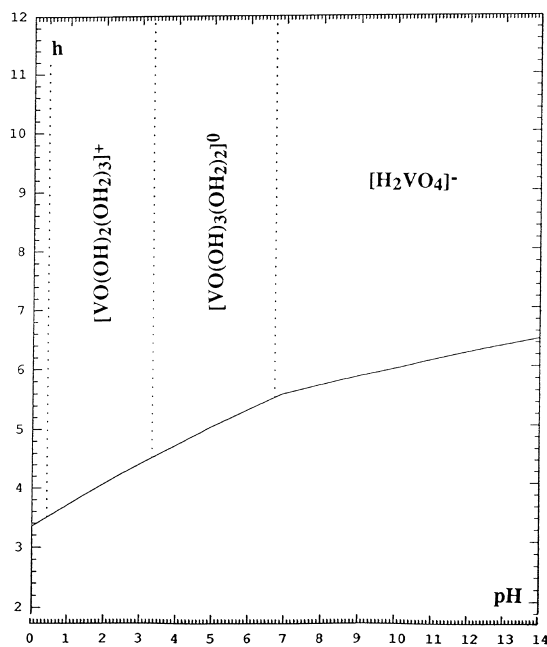
(b)

Fig. 1. V^V species in aqueous solutions: (a) experimental results as a function of pH and concentration; (b) hydrolysis ratio h as a function of pH deduced from the partial charge model (from ref. [8]).

are responsible for condensation:

$$\text{oxolation} \quad \text{V–OH} + \text{HO–V} \Rightarrow \text{V–O–V} + \text{H}_2\text{O} \tag{3}$$

$$\text{olation} \quad \text{V–OH} + \text{V–OH}_2 \Rightarrow \text{V–OH–V} + \text{H}_2\text{O} \tag{4}$$

The kinetics of olation mainly depend on the lability of coordinated water molecules. For d^0 cations such as V^V, these molecules are usually very labile and olation reactions are much faster than oxolation [8].

3. Condensation of vanadic acid

3.1. Ribbon-like vanadium pentoxide gels, $V_2O_5 \cdot nH_2O$

Vanadium pentoxide V_2O_5 can be precipitated from aqueous solutions around the point of zero charge ($h = 5$, pH ≈ 2). In order to avoid the presence of foreign ions, the acidification of an aqueous solution of sodium metavanadate, $NaVO_3$ (1 M, pH ≈ 9) was performed with a proton exchange resin (Dowex 50WX2, 50–100 mesh) [11]. The solution turns yellow as soon as acidification occurs, suggesting that the coordination of V^V increases from four to six. This clear solution turns orange and red upon aging, while its viscosity progressively increases. A dark red gel is obtained after a few hours. Precipitation is not observed, and the gel remains stable for years when kept in a closed vessel. A $V_2O_5 \cdot nH_2O$ ($n \approx 1.8$) xerogel is obtained upon drying in air at room temperature. Dehydration remains reversible as long as the sample is not heated above 150 °C and a gel is again formed when water is slowly added to the xerogel. Deep red colloidal solutions are obtained in the presence of a large excess of water ($n > 250$).

The ^{51}V NMR spectrum of the acid solution (pH ≈ 2) obtained after ion exchange shows the presence of two main species, decavanadic acid $[H_2V_{10}O_{28}]^{4-}$ and $[VO_2]^+$ [Fig. 2(a)]. NMR peaks progressively broaden and then disappear when the gel forms, but no other chemical species can be detected [12]. However, none of these species can be a precursor for vanadium oxide gels. They do not contain any stable V–OH group and further condensation cannot occur. The decavanadate ion should mainly behave as a reservoir for V^V ions via rapid dissociation–association reactions [13,14]. We may assume that the molecular precursor for V_2O_5 should be the neutral species $[VO(OH)_3(OH_2)_2]^0$ corresponding to $h = 5$. It readily leads to condensation and its lifetime should be too short for NMR observation.

This six-fold coordinated V^V precursor can be formed from the tetrahedral vanadic acid H_3VO_4, via the addition of two water molecules as suggested by the yellow coloration of the solution upon acidification. One water molecule lies along the "z" axis, opposite to the V=O double bond, while the other one lies in the equatorial plane [Fig. 3(a)]. Condensation cannot occur along the z direction (H_2O–V=O) as no V–OH group is present. It occurs only within the xy plane leading to a 2-D vanadium oxide network. However, both x and y directions are not equivalent toward condensation. Olation occurs along the H_2O–V–OH direction while oxolation goes on along the HO–V–OH direction. As olation reactions are usually faster
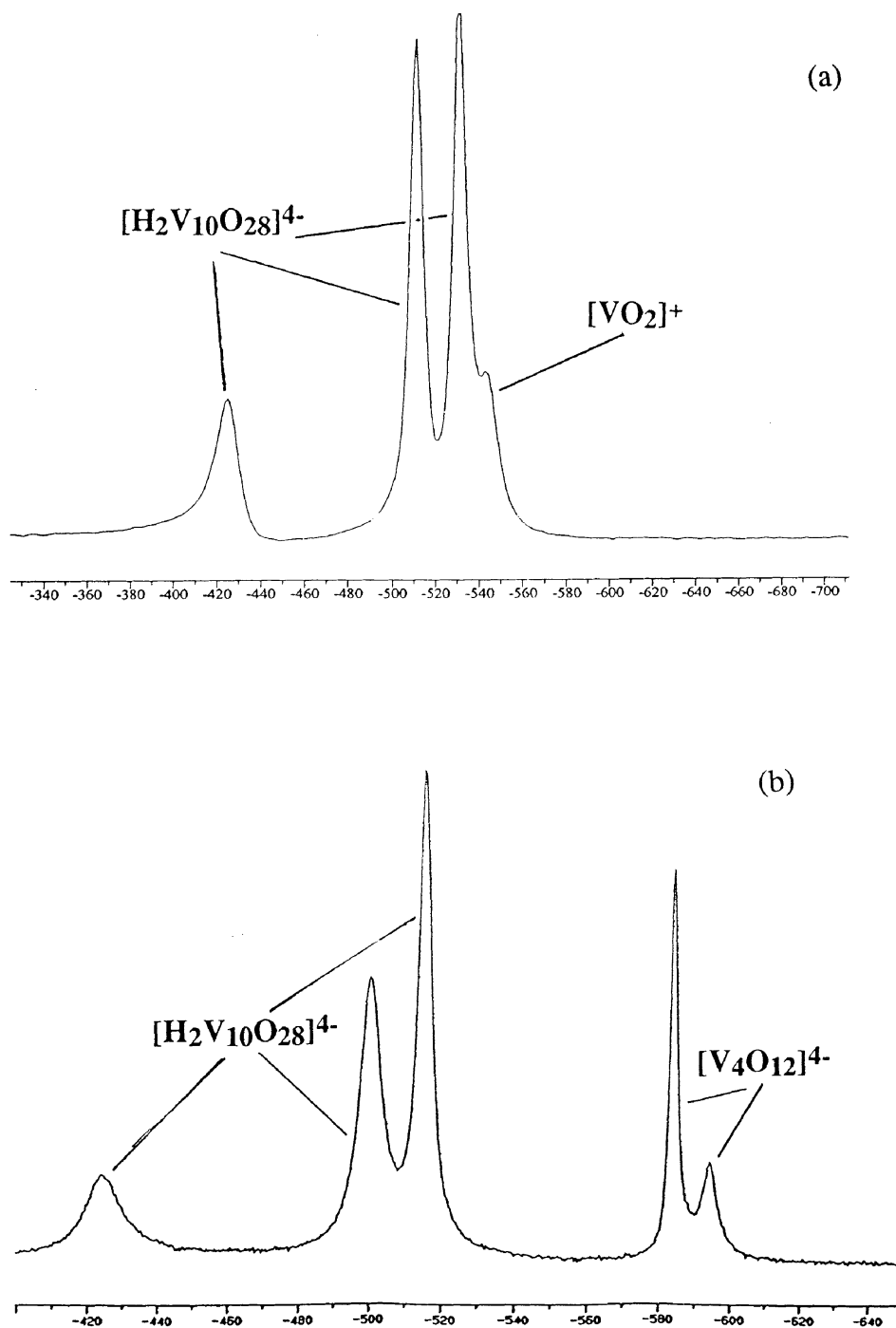
Fig. 2. ^{51}V NMR spectrum of aqueous solutions at different pH: (a) after acidification of a metavanadate solution (pH $\approx$ 2); (b) supernatant solution after the hydrothermal synthesis of polyoxovanadates from V$_2$O$_5$ and TMAOH (pH $\approx$ 6).
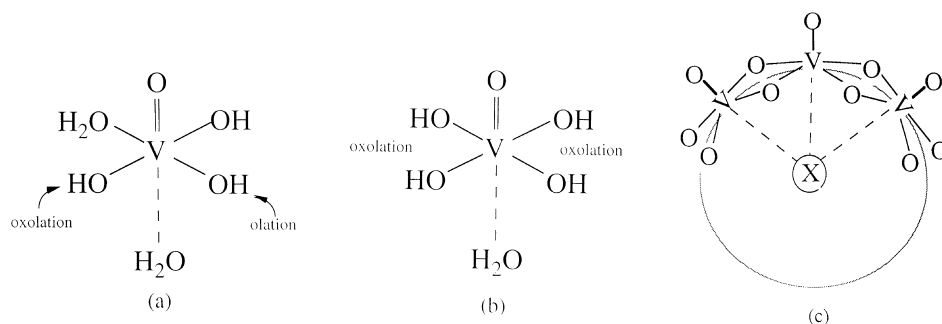
Fig. 3. Suggested V^V molecular precursors for the formation of solid phases: (a) neutral precursor $[VO(OH)_3(OH_2)_2]^0$ for $V_2O_5 \cdot nH_2O$ gels; (b) anionic precursor $[VO(OH)_4(OH_2)]^-$ for polyoxovanadates; (c) templating effect of anionic species X^-.

than oxolation, it may be assumed that ribbon-like particles rather that platelets would be formed, as confirmed by transmission electron microscopy (Fig. 4). These ribbons are about 0.5 μm long, 100 Å wide and 10 Å thick.

3.2. Vanadium oxide mesophases

When dispersed in an aqueous medium, vanadium oxide gels exhibit acid properties. Due to the strong polarizing power of V^{5+} ions, acid dissociation of V–OH
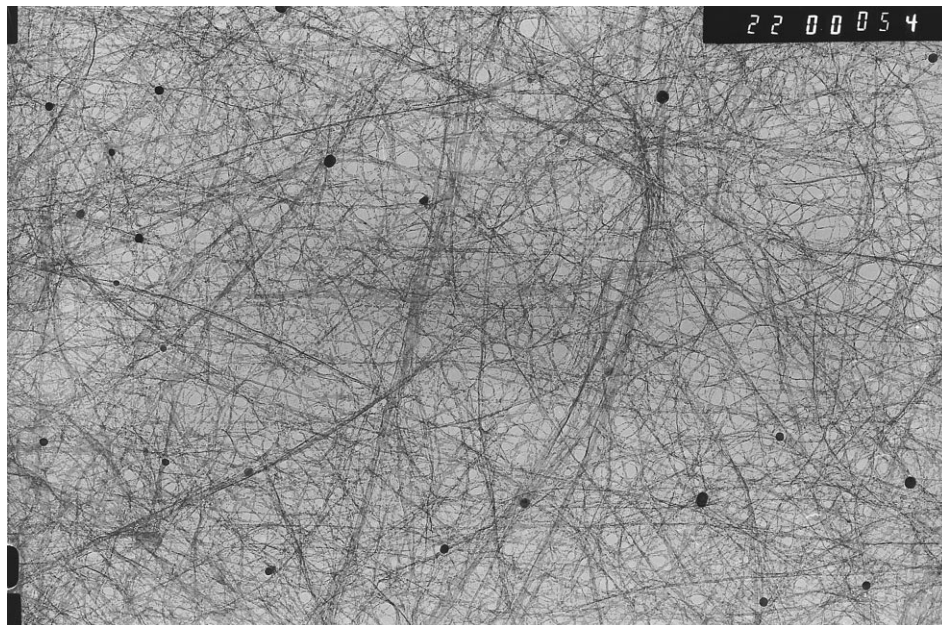

Fig. 4. Ribbon-like structure of vanadium pentoxide gels as shown by transmission electron microscopy (the bar corresponds to 0.1 μm).

groups occurs at the oxide/water interface as follows:

$$\rangle V\text{–OH} + H_2O \Leftrightarrow \rangle V\text{–O}^- + H_3O^+ \tag{5}$$

Vanadium oxide gels then behave as "polyoxovanadic acids" $H_xV_2O_5 \cdot nH_2O$. Protometric titration shows that about 0.3 protons per unit formula V_2O_5 are ionized at $pH \approx 2$ ($x \approx 0.3$). Vanadium oxide ribbons then bear the corresponding negative charge. Electrostatic repulsion prevents the precipitation of V_2O_5 and is responsible for the stabilization of $V_2O_5 \cdot nH_2O$ gels.

The liquid crystal behavior of vanadium oxide gels and sols was recently described by P. Davidson at the University of Orsay [15]. This is one of the very few examples of inorganic liquid crystals [16]. When observed by optical microscopy between crossed polarizers, vanadium oxide sols and gels display optical textures typical of nematic liquid crystals. These textures arise from the formation of topological defect lines called disclinations. A typical "banded texture" of a V_2O_5 gel is shown in Fig. 5. It is made of regularly spaced dark bands lying perpendicular to the shear flow direction. The dark brushes correspond to the regions where the ribbons are either parallel or perpendicular to the polarizer axis. Such a texture is currently displayed by nematic polymers such as hydroxypropyl cellulose or DNA. It points out the similarity of V_2O_5 sols with nematic solutions of semi-rigid polymers and confirms that the length of the ribbons is at least one order of magnitude larger than their width [17]. Recent experiments have shown that, in diluted sols, vanadium oxide ribbons can be oriented in any direction by applying a magnetic field as low as 0.2 T. This is due to the strong diamagnetic anisotropy of the ribbons and their cooperative behavior in nematic sols [18].
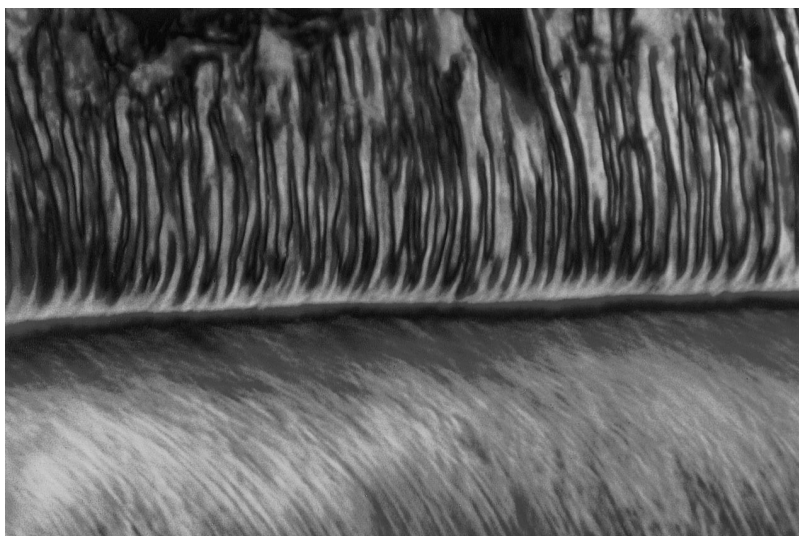

Fig. 5. Nematic texture of $V_2O_5 \cdot nH_2O$ gels observed between crossed polarizers.

3.3. Intercalation properties of vanadium pentoxide gels

The nematic ordering can be preserved upon drying. When deposited onto a flat substrate, vanadium pentoxide gels give rise to xerogel layers that exhibit some preferred orientation. X-ray diffraction of these xerogels display the 00l peaks typical of a turbostratic stacking of the V_2O_5 ribbons along a direction perpendicular to the substrate (Fig. 6). The 1-D Patterson map suggests that an oxide layer is made of two "V_2O_5" sheets facing each other at a distance of 2.8 Å [19]. However, contrary to V_2O_5 where V=O bonds are alternatively up and down in adjacent edge-sharing [VO_5] pyramids, all V=O bonds are "up" in one sheet and "down" in the other. Double layer structures are frequently encountered in vanadium oxide bronzes such as δ-$Ag_xV_2O_5$ [20]. Water molecules are intercalated between these ribbons and the basal distance increases by steps of about 2.8 Å when the amount of water increases ($d=8.7$ Å for $n=0.5$ and $d=11.5$ Å for $n=1.8$) [21].

Layered $V_2O_5 \cdot nH_2O$ gels have been shown to behave as a versatile host structure for intercalation [22]. V_2O_5 ribbons are linked together via hydrogen bonded water molecules. The basal distance is quite large and interactions between ribbons are much weaker than in crystalline V_2O_5. Intercalation reactions are then much faster. They proceed at room temperature within minutes rather than hours. Intercalation can be followed easily by X-ray diffraction via the variation of the basal spacing. The driving force for intercalation is mainly based on ion exchange reactions between acid protons within the gel and foreign cations in the solution. However, molecular exchange with intercalated water molecules or electron exchange via V^{5+}/V^{4+} reduction can also be involved in these reactions. A wide range of ionic (metal ions,
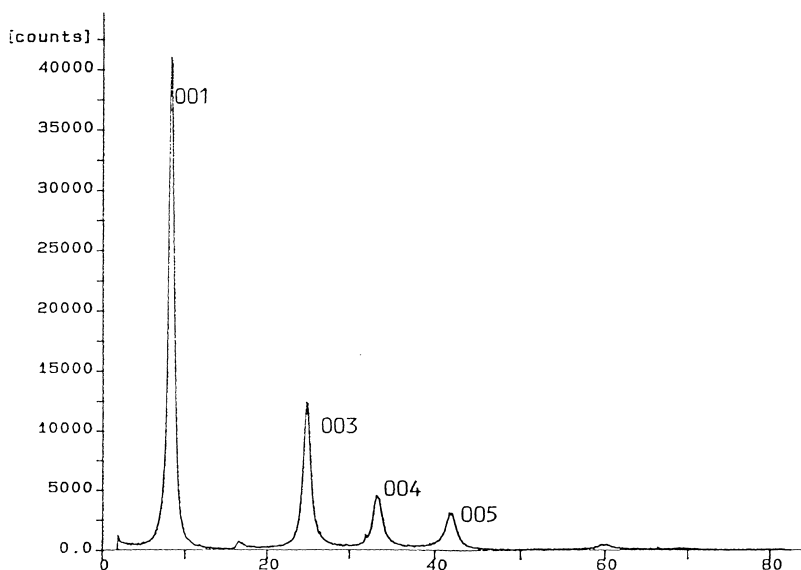

Fig. 6. X-ray diffraction pattern of a $V_2O_5 \cdot nH_2O$ xerogel thick film ($n=1.8$, $d=11.5$ Å).

alkylammonium cations) or molecular (organic molecules) species have been intercalated within these gels by our group in Paris [23].

The facile intercalation of organic molecules within the layered structure of $V_2O_5 \cdot nH_2O$ gels leads to a whole range of hybrid materials. The intercalation of organic monomers such as aniline, pyrrole or thiophene, followed by their in situ oxidative polymerization, leads to a new class of nanocomposites in which a variety of electronically conducting organic polymers are inserted between the 2-D structure of the oxide layers [24,25]. These nanocomposites show improved room temperature conductivity and could be used as cathodes in lithium batteries [26,27]. Polyethylene oxide has also been intercalated within V_2O_5 gels, giving mixed ionic–electronic conducting nanocomposites [28,29].

4. Condensation of anionic precursors

4.1. Chain and cyclic metavanadates

Anionic precursors $[H_nVO_4]^{(3-n)-}$ are formed above the point of zero charge (pH ≈ 2) leading to negatively charged polyanions. Cations have then to be added to the solution in order to precipitate solid vanadates.

The oxo-anion $[VO_4]^{3-}$ in which V^V is surrounded by four equivalent oxygen atoms is observed at very high pH only. There is no functional V–OH group, V–O–V bonds cannot be formed and only orthovanadates containing isolated $[VO_4]$ tetrahedra can be obtained above pH ≈ 12. Protonation occurs at lower pH, giving $[H_nVO_4]^{(3-n)-}$ species. The condensation of monofunctional $[HVO_4]^{2-}$ is limited to dimeric pyrovanadates $[V_2O_7]^{4-}$ made of two corner-sharing tetrahedra ($9 \leqslant pH \leqslant 14$).

The difunctional precursor $[H_2VO_4]^-$ leads to more condensed metavanadates. In the pH range 6–9, metavanadates form cycles and chains. Cyclic species such as $[V_4O_{12}]^{4-}$ are usually observed in the solution were they can be evidenced by ^{51}V and ^{17}O NMR [30], whereas chain metavanadates, $[VO_3^-]_n$, are currently formed in the solid state. They are built up of single chains of corner-sharing $[VO_4]$ tetrahedra as in KVO_3 or double chains of edge-sharing $[VO_5]$ trigonal bipyramids in $KVO_3 \cdot H_2O$ [31].

The metavanadate salt of ter-butylammonium is specially interesting. Depending on synthesis temperature, both cyclic $[(CH_3)_3CNH_3]_4[V_4O_{12}]$ and chain $[(CH_3)_3CNH_3][VO_3]$ metavanadates can be synthesized from aqueous solutions. This is the first example of a solid polyoxovanadate precipitated from an aqueous solution containing a discrete unprotonated $[V_4O_{12}]^{4-}$ cyclic anion [32,33]. Moreover, a phase transition from cyclic to chain has been observed in the solid state [34].

Vanadium coordination increases up to six at lower pH (pH <6). The solution turns from colorless to orange and decavanadate anions such as $[H_2V_{10}O_{28}]^{4-}$ made of 10 edge-sharing $[VO_6]$ octahedra are formed. These decavanadic species are strong acids, further condensation does not occur and $[H_nV_{10}O_{28}]^{(6-n)-}$ cannot be a precursor for more condensed species. In this pH range, the formation of a solid network

is obtained when cations are added to the solution, leading to the precipitation of decavanadate salts such as $[(CH_3)_3CNH_3][V_{10}O_{28}] \cdot 8H_2O$ [35].

4.2. Layered polyoxovanadates

Layered polyoxovanadates have been precipitated in the presence of large organic cations such as tetramethyl ammonium, $[TMA]^+ = [N(CH_3)_4]^+$. They are usually obtained by hydrothermal synthesis at a pH close to 7. In our experiments, V_2O_5 (≈ 1 g) was mixed with an aqueous solution of 1 M TMAOH (≈ 5 ml) in a Teflon lined autoclave (Parr bomb) and heated at 200 °C for 48 h under autogenous pressure. Black crystals of $N(CH_3)_4[V_4O_{10}]$ are formed [Fig. 7(a)]. Their structure was described recently by Whittingham and coworkers [36]. It is close to that of orthorhombic V_2O_5. The $[V_4O_{10}]^-$ anionic layers are made up of double chains of edge-sharing $[VO_5]$ tetragonal pyramids linked together by corners [Fig. 7(b)]. Large alkylammonium cations are distributed between the oxide layers.

Before the reaction the pH of the solution is close to 13, leading to the dissolution of V_2O_5 and the formation of vanadate ions $[VO_4]^{3-}$ as follows:

$$V_2O_5 + 6OH^- \Rightarrow 2[VO_4]^{3-} + 3H_2O \qquad (6)$$

The pH decreases during dissolution and protonated species, $[H_nVO_4]^{(3-n)-}$, are formed, allowing condensation to take place via oxolation. The ^{51}V NMR spectrum of the supernatant solution after hydrothermal reaction (pH ≈ 6) exhibits two series of peaks corresponding to a mixture of metavanadates $[H_nV_4O_{12}]^{(4-n)-}$ and decavanadates $[H_nV_{10}O_{28}]^{(6-n)-}$ [Fig. 2(b)]. The relative intensities of metavanadate and decavanadate NMR peaks depend on the pH of the solution. Metavanadate species decrease and only decavanadates are observed below pH ≈ 6.

As for vanadium oxide gels, it has to be pointed out that vanadate species in the solid phase are different from those found in the solution, $[H_nV_4O_{12}]^{(4-n)-}$ and $[H_nV_{10}O_{28}]^{(6-n)-}$. Neither the decavanadate nor the metavanadate anions can be molecular precursors for $N(CH_3)_4[V_4O_{10}]$. Therefore, the polyoxovanadate network $[V_4O_{10}]^-$ might be formed from the anionic $[VO(OH)_4(OH_2)]^-$ precursor [Fig. 3(b)]. As for the neutral precursor, no condensation is observed along the $H_2O-V=O$ direction. Oxolation reactions occur only in the equatorial plane along the four equivalent V–OH directions, leading to a truly 2-D polyoxovanadate network. Large alkylammonium cations behave as counter cations. They lie between the vanadate layers and interact with the negatively charged terminal oxygen ($V=O$). The formation of the oxide network is mainly governed by the dipolar interactions between adjacent $V=O$ bonds. The structure of these planes is close to that of V_2O_5. However, the $V=O$ bonds of two adjacent edge-sharing $[VO_5]$ pyramids are situated on the same side of the plane. This might be due to the large size of organic cations. The repulsion between adjacent $V=O$ is partially compensated by a tilt of the polyhedra, giving $[V_2O_8]$ units where $V=O$ bonds are alternatively "up" and "down".

The pH of the solution should be a major parameter, as another compound,

(b)

(a)
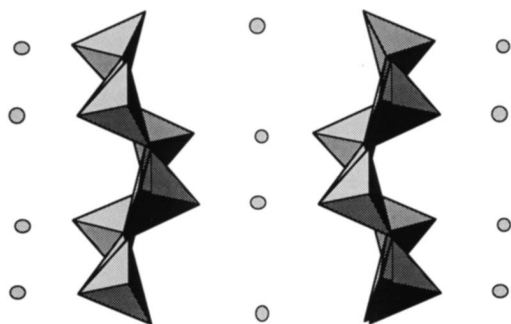
Fig. 7. Crystals of $N(CH_3)_4[V_4O_{10}]$: (a) scanning electron microscopy; (b) layered structure (from ref. [36]).

TMAV$_3$O$_7$, was obtained at higher pH (pH $\approx$ 8) by Whittingham and coworkers [37]. At such a pH tetrahedral precursors could also be involved in the formation of the polyvanadate network. Its structure is then made of zig-zag strings of edge-sharing [V^{IV}O$_5$] pyramids joined together by [V^{V}O$_4$] tetrahedra [38]. This structure is close to that of [HN(C$_2$H$_4$)$_3$NH][V$_6$O$_{14}$]·H$_2$O obtained in the presence of DABCO (1,4-diazabicyclo[2.2.2]octane) [39,40]. The main difference is that the sheets of the hexavanadate synthesized by Nazar et al. are highly puckered while they are planar with TMA. Moreover, once DABCO has been removed, the vanadate network can reversibly intercalate up to 8 Li/mol V$_6$O$_{14}$ [39]. This does not seem to be possible with TMA[V$_3$O$_7$] as long as the organic cation has not been removed. Another compound, TMAV$_8$O$_{20}$, is formed at lower pH (pH $\approx$ 3), not far from the point of zero charge. Like V$_2$O$_5$ gels, it is made of ribbon-like particles. However, the presence of organic cations leads to some vanadium reduction (V^{4+}/V^{5+} = 1/7) and the lower charge of V^{4+} ions is compensated by TMA$^+$ [41].

The hydrothermal synthesis of layered polyoxovanadates in the presence of amines has been extensively studied during the past few years. As for many microporous compounds, these amines were supposed to act as templating agents. Actually this does not seem to be the case as layered structures are currently obtained. The pH of the solution appears to be more important, as shown by the syntheses performed in the presence of diamines H$_2$N(CH$_2$)$_n$NH$_2$ by D. Riou at the University of Versailles [42,43]. According to the authors, the final pH is the same in all experiments (pH $\approx$ 5), but before reaction, the pH is 4 for diaminopropane (n = 3) and 9 for diaminobutane (n = 4). The first compound contains mixed valence [V$_4$O$_{10}$]$^{2-}$ layers built of [V^{V}O$_4$] tetrahedra and pairs of edge-sharing [V^{IV}O$_5$] pyramids [42,44]. The second compound is a chain metavanadate [VO$_3^-$]$_n$ formed of corner-sharing [V^{V}O$_4$] tetrahedra [43,45]. The higher pH favors the oxidation of V^{IV} into V^V and the formation of tetrahedral [H$_n$VO$_4$]$^{(3-n)-}$ precursors. In both cases, protonated diamines are situated between the oxide layers or chains.

4.3. Polyoxovanadate clusters

The previous examples suggest that organic cations do not behave as templating agents during the hydrothermal synthesis of polyoxovanadates. Layered or chain structures are formed as with the usual inorganic cations. Organic species should simply act as reducing agents and most of the compounds described above are mixed valence vanadates containing both V^V and V^{IV} oxidation states. Unexpectedly, as shown by Müller and coworkers [3,5], anions rather than cations behave as structure directing agents, leading to the formation of hollow clusters of polyoxovanadates in which many anionic species can be inserted.

The syntheses described in the literature are sometimes quite complicated, and the link between reagents and the resulting compound is not always obvious. We have shown that cluster shell oxopolyvanadates can be formed in a very simple manner via the hydrothermal treatment (200 °C, 48 h) of a mixture of V$_2$O$_5$ ($\approx 5 \times 10^{-3}$ mol), NMe$_4$X (X = Cl, I) ($\approx 2 \times 10^{-3}$ mol) and NMe$_4$OH (5×10^{-3} mol) [46]. As for NMe$_4$[V$_4$O$_{10}$], the pH of the solution decreases from 13

to about 7 during the hydrothermal synthesis. Black crystals are formed and the supernatant solution contains a mixture of meta and decavanadate species. Hexagonal crystals are precipitated with X=Cl [Fig. 8(a)]. They have the same structure as the $(NMe_4)_6[V_{15}O_{36}Cl] \cdot 4H_2O$ crystals synthesized by Müller using thiovanadates $[VS_4]^{3-}$ as precursors [47]. The hollow anion $[V_{15}O_{36}]^{5-}$ is made of tetragonal $[VO_5]$ pyramids sharing edges and corners [Fig. 8(b)]. Vanadium atoms are placed at the surface of a sphere at a distance $Cl \cdots V \approx 3.43$ Å from the center of the cluster where the entrapped Cl^- anion resides. All short V=O bonds are oriented toward the outside of the sphere. Some vanadium reduction occurs during the reaction and the $[V_{15}O_{36}Cl]^{6-}$ anion is a mixed valence compound containing seven V^V and eight V^{IV}.

Octahedral black crystals are formed in the same conditions with I^- [Fig. 9(a)]. They are made of $[V_{18}O_{42}I]$ anionic spheres similar to those found for the cesium salt $Cs_9[H_4V_{18}O_{42}I] \cdot 12H_2O$ synthesized by Müller in the presence of HI and N_2H_4OH as a reducing agent [48,49]. According to thermal and chemical analyses, our compound should rather correspond to $(NMe_4)_{10}[H_3V_{18}O_{42}I] \cdot 3H_2O$ and all vanadium are in the V^{IV} oxidation state. The $[V_{18}O_{42}]^{12-}$ hollow sphere is built from $[VO_5]$ square pyramids sharing edges. Vanadium atoms are at an average distance $I \cdots V \approx 3.75$ Å from the central encapsulated I^-. As previously, all short V=O double bonds are opposite to the encapsulated anion [Fig. 9(b)].

A large number of hollow polyoxovanadate clusters have been synthesized during the past few years [3–6]. They may contain as many as 34 vanadium atoms in $K_{10}[V_{34}O_{82}] \cdot 20H_2O$ formed by linking 30 tetragonal pyramids $[VO_5]$ and a central $[V_4O_4]O_4$ cube [50].

As shown by Bénard and coworkers [51] and Henry and coworkers [46] in Strasbourg, interactions between the central anion and the negatively charged poly-oxovanadate cage are very weak. The vanadate cage is mainly polarized by the central anion so that the negative density is pushed toward the V=O pointing outside of the cage where they interact with the positive cations. The parameters for the CERIUS force field have been derived from structural data of 15 polyoxovana-date clusters and cages [52].

Hollow clusters $[V_{15}O_{36}Cl]^{6-}$ and $[V_{18}O_{42}I]^{13-}$ are formed in the same conditions as the layered vanadates $[V_4O_{10}]^-$. It may then be assumed that they are formed from the same precursor $[VO(OH)_4(OH_2)]^-$ [Fig. 3(b)]. The polyoxovanadate net-work V–O–V is built via the condensation of V–OH groups in the equatorial plane leading to 2-D compounds made of corner- and edge-sharing $[VO_5]$ pyramids. The way these pyramids are linked together should depend on the nature of the other ionic species in the solution.

Large and weakly polarizing tetramethyl cations ($r_{TMA^+} = 3.47$ Å) interact weakly with the negative oxygen of terminal V=O. They behave as counter cations rather than templates in order to form a neutral solid with the negatively charged polyoxo-vanadate network. In the absence of smaller ions, the main interactions are between adjacent V=O dipoles. They lead to a layered structure with half of the $[VO_5]$ pyramids "up" and the other half "down". The space between these layers is
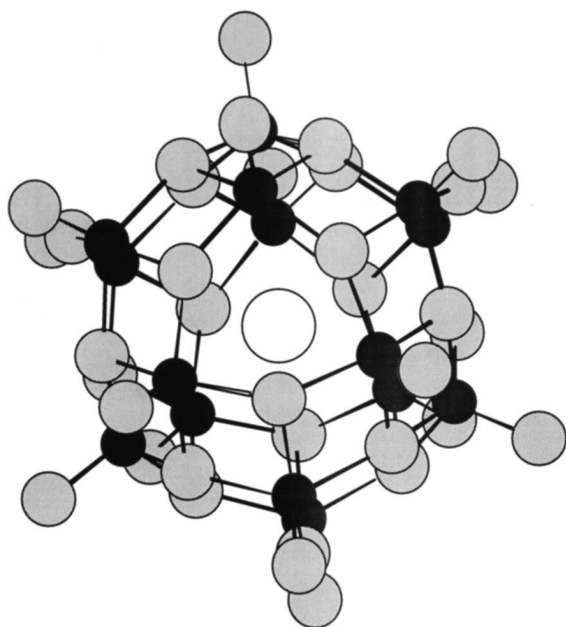
(b)
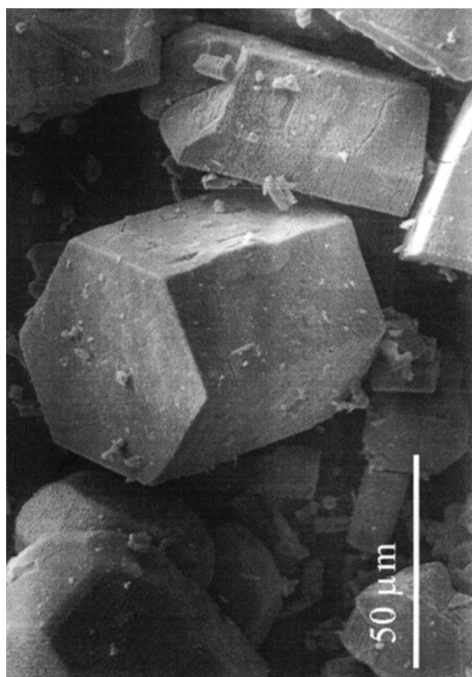
(a)

Fig. 8. Cluster shell polyoxovanadate $(NMe_4)_6[V_{15}O_{36}Cl]4H_2O$: (a) scanning electron microscopy; (b) molecular structure (from ref. [47]).

(b)

(a)
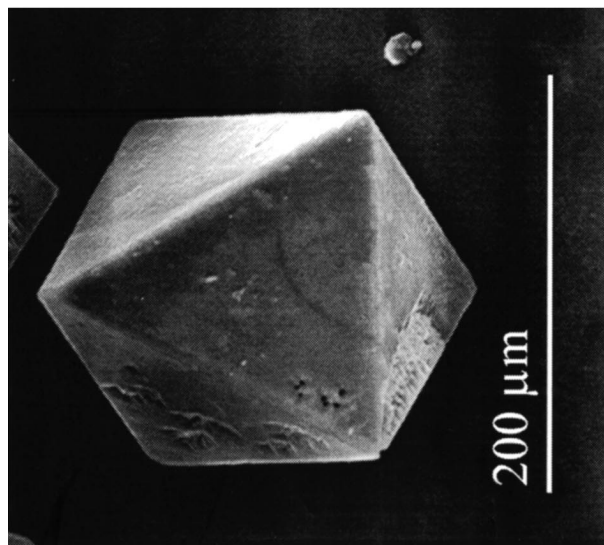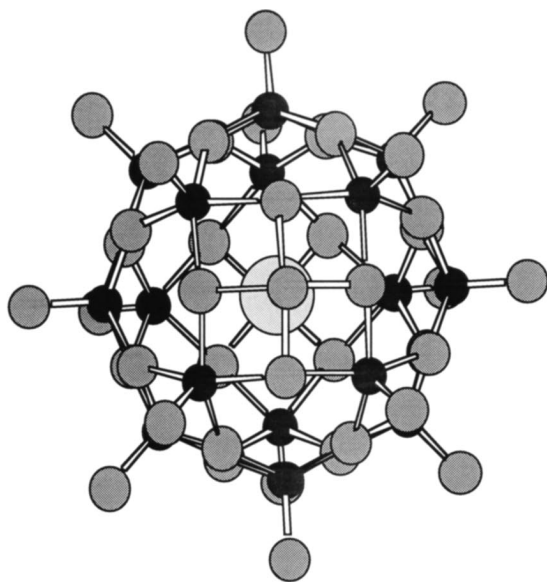
Fig. 9. Cluster shell polyoxovanadate $(NMe_4)_{10}[H_3V_{18}O_{42}I]3H_2O$: (a) scanning electron microscopy; (b) molecular structure (from ref. [48]).

occupied by $[NMe_4]^+$ ions. Similar structures are formed in the presence of large protonated amines.

Cluster shell species are formed in the presence of X^- anions that should behave as templates during the formation of the polyoxovanadate network. Encapsulated anions are smaller and more polarizing than the tetramethyl cation ($r_{Cl^-} = 1.81$ Å, $r_{I^-} = 2.16$ Å). Dipolar interactions between adjacent V=O do not prevail any longer, and anions appear to control the formation of the surrounding cluster shell. This should be due to the particular geometry of $[VO_5]$ pyramids in which the water molecule $V\cdots OH_2$ opposite to the V=O bond is very labile. Negative anions X^- can then interact with the positive $V^{\delta+}$, favoring the formation of spherical species around a central anion [Fig. 3(c)]. All V=O dipoles are then oriented toward the outside of the shell where they repel each other, favoring the formation of convex surfaces. They interact weakly with large organic counter cations. Electrostatic attractions between big anionic polyvanadates and organic cations lead to the crystallization of hybrid "ionic" crystals with large cell parameters. The greater size and reducing power of I^- ($Cl^-/Cl = 1.36$ V, $I^-/I = 0.54$ V) should be responsible for the formation of the fully reduced $[V_{18}O_{42}I]^{13-}$ cluster instead of the mixed valence one $[V_{15}O_{36}Cl]^{6-}$. I_2 is even formed when NMe_4I is in excess. It has to be pointed out that a $[V_{18}O_{42}Cl]^{13-}$ cluster was also synthesized by Yamase et al. at room temperature, but the experimental conditions were different. It was obtained via photochemical reduction under UV irradiation in a neutral atmosphere [53]. The presence of reduced V^{4+} ions seems to be a requirement for the clusters to be formed. A large number of mixed valence polyoxovanadate clusters was recently synthesized by Müller et al. starting from V^{IV} precursors rather than V^V [54].

It might be interesting to point out that completely different structures are formed when other ions are added to the solution before hydrothermal synthesis. A mixture of $V_2O_5 + NMe_4OH + NMe_4I$ leads to the cluster compound $(NMe_4)_{10}[H_3V_{18}O_{42}I] \cdot 3H_2O$ while, in the same conditions, replacing NMe_4I by KI leads to the precipitation of the mixed valence compound $K_2V_3O_8$. Interactions of the smaller and more polarizing K^+ ($r_{K^+} = 1.33$ Å) with the vanadium precursor prevail. As with other positive ions, a layered structure is formed. It is built of $[V^{IV}O_5]$ pyramids and pairs of corner-sharing $[V^VO_4]$ tetrahedra. K^+ cations are intercalated between the $[V_3O_8]^{2-}$ layers [55]. Large NMe_4^+ and I^- ions remain in the solution and are no longer involved in the formation of the solid phase. The reducing role of the organic cation can be clearly evidenced. A fully oxidized potassium vanadate KV_3O_8 is formed when NMe_4OH is replaced by KOH.

5. Conclusion

A large variety of polyoxovanadates can be synthesized from aqueous solutions and this paper shows that small changes in the synthesis conditions can lead to completely different compounds. From this survey, it appears that the molecular structure of the V^V precursor depends mainly on pH, but the way these precursors

self-assemble to give a vanadium oxide network may be governed by the other ionic species in the solution.

V^V molecular precursors result from the hydrolysis of V^{5+} ions in water (deprotonation of coordinated water molecules). Six-fold coordinated species $[V(OH)_h(OH_2)_{6-h}]^{(5-h)+}$ ($h = 4, 5$) are formed in acid solutions while four-fold coordinated vanadates $[H_nVO_4]^{(3-n)-}$ are observed at neutral or alkaline pH (Fig. 1). Specially interesting is the pH range where coordination changes from 6 to 4. A large variety of different structures built up of $[VO_6]$, $[VO_5]$ and $[VO_4]$ units can then be obtained around pH $\approx$ 6–8. In this paper we suggest that the vanadium oxide network could be formed via the condensation of $[VO(OH)_3(OH_2)_2]^0$ or $[VO(OH)_4(OH_2)]^-$ precursors (Fig. 3), despite the fact that such species have never been evidenced in aqueous solutions. Over the whole range of pH, ^{51}V NMR spectra only show peaks corresponding to $[VO_2]^+$, decavanadate and cyclic metavanadate species (Fig. 2). This might be due to the very short lifetime of such precursors. Condensation occurs readily so that their concentration as isolated species in the solution always remains at a very low level.

Weak interactions between solute species (hydrogen bonds, van der Waals, hydrophilic–hydrophobic interactions, etc.) are not broken by the mild conditions associated with "chimie douce". They are involved in the formation of supramolecular assemblies and foreign ions (cations and anions) may govern the way V^V molecular precursors are linked together via condensation. In the case of $[VO(OH)_4(OH_2)]^-$, oxolation reactions in the equatorial plane lead to the formation of 2-D structures. In the absence of other ions or with large and weakly charged cations such as $[N(CH_3)_4]^+$, dipolar repulsion between V=O groups prevails, leading to layered structures in which V=O are alternatively up and down. Cationic species are intercalated between these layers where they interact with the negative oxygen of V=O.

Condensation cannot occur along the H_2O–V=O direction (Fig. 3). However, the water molecule is weakly bonded and highly labile. The positively charged $V^{\delta+}$ ion therefore becomes accessible to anions that can behave as templating agents. They lead to the formation of closed vanadate shells [Fig. 3(c)]. This is no longer the case for tetrahedral $[VO_4]$ or octahedral $[VO_6]$ basic units in which vanadium is protected by the surrounding oxygen atoms.

The way the $[VO_5]$ primary building units self-assemble results from a competition between all ionic species. It seems to be mainly governed by the polarizing power (size and charge) of the different ions. Large NMe_4^+ cations are not involved in the formation of the vanadate network in the presence of smaller cations such as Li^+ or K^+ [55]. They only behave as counter ions in the presence of Cl^- or I^-. The templating behavior of these anions does not stand any longer when smaller cations are present in the solution. The hydrothermal treatment of a mixture of V_2O_5, TMAOH and KI leads to the formation of $K_2V_3O_8$. Large TMA^+ and I^- ions remain in the solution and do not participate in the formation of the solid phase.

The competition between ions to form self-assemblies does not depend on their size and charge only. The interaction of cations with V=O and that of anions with $V^{\delta+}$ cannot be compared in a straightforward manner. Many other parameters

should also be taken into account, but most experimental procedures published in the literature do not give enough information, even the pH of the solution is often not given.

The nature of the molecular precursor may also depend on the redox potential of the aqueous solution. Such a parameter is usually not taken into account in the literature. However, it is well known that V^{5+} ions can easily be reduced into V^{4+}. New $[V(OH)_h(OH_2)_{6-h}]^{(4-h)+}$ precursors are then formed. V^{4+} ions are larger than V^{5+} and never exhibit tetrahedral coordination. Only $[V^{IV}O_6]$ and $[V^{IV}O_5]$ units are formed. The aqueous chemistry of V^{4+} has not been so widely studied as the aqueous chemistry of V^{5+}. The vanadyl ion $[VO(OH_2)_5]^{2+}$ or $[VO]^{2+}$ is formed at low pH, while $VO(OH)_2$ precipitates around $pH \approx 7$. V^{IV} compounds are soluble in alkaline medium but as the V^{4+}/V^{5+} potential depends on pH, they are then readily oxidized in air:

$$[VO]^{2+} + H_2O \Leftrightarrow [VO_2]^+ + e^- + 2H^+ \tag{7}$$

This explains why so many mixed valence compounds are obtained in the presence of reducing species. This is also the reason why V^{IV} precursors ($VOSO_4 \cdot nH_2O$) have been used for the synthesis of vanadium oxide bronzes [56]. The higher coordination of V^{IV} above $pH \approx 7$ favors the condensation of $[VO_5]$ units. It is even possible to avoid hydrothermal conditions and perform the reaction at room temperature in the presence of hydrazine [54,57] or under photochemical reduction [53].

Care has also to be taken when syntheses are performed under hydrothermal conditions. The viscosity and dielectric constant of water decrease when the temperature increases. At 200 °C, for instance, the dielectric constant of water is close to 30 instead of 80 at room temperature. Ionic associations are different at higher temperatures and the pH scale of aqueous solutions is narrower. The aqueous chemistry of cations in hydrothermal conditions may then be quite different from that described at room temperature, but very little is known about this point.

References

[1] J. Gopalakrishnan, Chem. Mater. 7 (1995) 1265.
[2] M.T. Pope, Heteropoly and Isopoly Oxometalates, Inorganic Chemistry Concepts, vol. 8, Springer, Berlin, 1983.
[3] M.T. Pope, A. Müller, Angew. Chem., Int. Ed. Engl. 30 (1991) 34.
[4] J. Zubieta, Comm. Inorg. Chem. 16 (1994) 153.
[5] A. Müller, H. Reuter, S. Dillinger, Angew. Chem., Int. Ed. Engl. 34 (1995) 2328.
[6] M.I. Khan, J. Zubieta, Progr. Inorg. Chem. 43 (1995) 1.
[7] C.F. Baess, R.E. Mesmer, Hydrolysis of Cations, Wiley, New York, 1976.
[8] M. Henry, J.P. Jolivet, J. Livage, Structure and Bonding 77 (1992) 153.
[9] R.T. Sanderson, Science 114 (1951) 670.
[10] L. Pettersson, B. Hedman, I. Andersson, N. Ingri, Chem. Scripta 22 (1983) 254.
[11] N. Gharbi, C. Sanchez, J. Livage, J. Lemerle, L. Nejem, J. Lefebvre, Inorg. Chem. 21 (1982) 2758.
[12] G.A. Pozarnsky, A.V. McCornick, Chem. Mater. 6 (1994) 380.
[13] R.K. Murmann, K.C. Giese, Inorg. Chem. 17 (1978) 1160.
[14] P. Comba, L. Helm, Helv. Chim. Acta 71 (1988) 1406.

[15] P. Davidson, A. Garreau, J. Livage, Liquid Crystals 16 (1994) 905.
[16] P. Davidson, P. Batail, J.C. Gabriel, J. Livage, C. Sanchez, C. Bourgaux, Progr. Polym. Sci. 22 (1997) 913.
[17] P. Davidson, C. Bourgaux, L. Schoutteten, P. Sergot, C. Williams, J. Livage, J. Phys. II 5 (1995) 1577.
[18] X. Commeinhes, P. Davidson, C. Bourgaux, J. Livage, Adv. Mater. 9 (1997) 900.
[19] T. Yao, Y. Oka, N. Yamamoto, Mater. Res. Bull. 27 (1992) 669.
[20] J. Galy, J. Solid State Chem. 100 (1992) 229.
[21] P. Aldebert, N. Baffier, N. Gharbi, J. Livage, Mater. Res. Bull. 16 (1981) 669.
[22] P. Aldebert, N. Baffier, J.J. Legendre, J. Livage, Rev. Chim. Miner. 19 (1982) 485.
[23] J. Livage, Chem. Mater. 3 (1991) 578.
[24] M.G. Kanatzidis, C.G. Wu, H.O. Marcy, C.R. Kannewurf, J. Am. Chem. Soc. 111 (1989) 4139.
[25] C.G. Wu, D.C. DeGroot, H.O. Marcy, J.L. Schindler, C.R. Kannewurf, Y.J. Liu, W. Hirpo, M.G. Kanatzidis, Chem. Mater. 8 (1996) 1992.
[26] F. Leroux, B.E. Koene, L.F. Nazar, J. Electrochem. Soc. 143 (1996) L181.
[27] H.P. Wong, B.C. Dave, F. Leroux, J. Harreld, B. Dunn, L.F. Nazar, J. Mater. Chem., 8 (1998) 1019.
[28] Y.J. Liu, J.L. Schindler, D.C. DeGroot, C.R. Kannewurf, W. Hirpo, M.G. Kanatzidis, Chem. Mater. 8 (1996) 525.
[29] G.M. Kloster, J.A. Thomas, P.W. Brazis, C.R. Kannewurf, D.F. Shriver, Chem. Mater. 8 (1996) 2418.
[30] E. Heath, O.W. Howarth, J. Chem. Soc., Dalton Trans. (1981) 1105.
[31] H.T. Evans, Z. Krist. (1960) 257.
[32] P. Roman, A. San José, A. Luque, J.M. Gutiérez-Zorrilla, Inorg. Chem. 32 (1993) 775.
[33] M.-T. Averbuch-Pouchot, A. Durif, Eur. J. Solid State Inorg. Chem. 31 (1994) 567.
[34] A.S. Wéry, J.M. Gutiérez-Zorrilla, A. Luque, M. Ugalde, P. Roman, Chem. Mater. 8 (1996) 408.
[35] M.-T. Averbuch-Pouchot, Eur. J. Solid State Inorg. Chem. 31 (1994) 557.
[36] P.Y. Zavalij, M.S. Whittingham, E.A Boylan, Z. Krist. (1996) 211.
[37] T.G. Chirayil, E.A. Boylan, M. Mamak, P.Y. Zavalij, M.S. Whittingham, Chem. Commun. (1997) 33.
[38] E.A. Boylan, T. Chirayil, J. Hinz, P.Y. Zavalij, M.S. Whittingham, Solid State Ionics 90 (1996) 1.
[39] L.F. Nazar, B.E. Koene, J.F. Britten, Chem. Mater. 8 (1996) 327.
[40] Y. Zhang, R.C. Haushalter, A. Clearfield, Chem. Commun. (1996) 1055.
[41] T. Chirayil, P.Y. Zavalij, M.S. Whittingham, J. Mater. Chem. 7 (1997) 2193.
[42] D. Riou, G. Ferey, J. Solid State Chem. 120 (1995) 137.
[43] D. Riou, G. Ferey, J. Solid State Chem. 124 (1996) 151.
[44] Y. Zhang, C.J. O'Connor, A. Clearfield, R.C. Haushalter, Chem. Mater. 8 (1996) 595.
[45] Y. Zhang, R.C. Haushalter, A. Clearfield, Inorg. Chem. 35 (1996) 4950.
[46] J. Livage, L. Bouhedja, C. Bonhomme, M. Henry, Mater. Res. Soc. Symp. Proc. 457 (1997) 13.
[47] A. Müller, E. Krickmeyer, M. Penk, H.J. Walberg, H. Bögge, Angew. Chem., Int. Ed. Engl. 26 (1987) 1045.
[48] A. Müller, M. Penk, R. Rohling, E. Krickmeyer, J. Döring, Angew. Chem., Int. Ed. Engl. 29 (1990) 926.
[49] G.K. Johnson, E.O. Schlemper, J. Am. Chem. Soc. 100 (1978) 3645.
[50] A. Müller, R. Rohlfing, J. Döring, M. Penk, Angew. Chem., Int. Ed. Engl. 30 (1991) 588.
[51] M.M. Rohmer, J. Devény, R. Wiest, M. Bénard, J. Am. Chem. Soc. 118 (1996) 13007.
[52] C. Menke, E. Diemann, A. Müller, J. Mol. Struct. 436437 (1997) 35.
[53] T. Yamase, K. Ohtaka, M. Suzuki, J. Chem. Soc., Dalton Trans. (1996) 283.
[54] A. Müller, R. Sessoli, E. Krickemeyer, H. Bögge, J. Meyer, D. Gatteschi, L. Pardi, J. Westphal, K. Hovemeier, R. Rohlfing, J. Döring, F. Hellweg, C. Beugholt, M. Schmidtmann, Inorg. Chem. 36 (1997) 5239.
[55] T. Chirayil, P. Zavalij, M.S. Whittingham, Solid State Ionics 84 (1996) 163.
[56] Y. Oka, T. Yao, N. Yamamoto, O. Tamada, Mater. Res. Bull. 32 (1997) 59.
[57] E. Dumas, C. Livage, S. Halut, G. Hervé, Chem. Commun. (1996) 2437.